MNRAS **000**, 1–15 (0000) Preprint 5 June 2023 Compiled using MNRAS LATEX style file v3.0

What insights can be gained into the formation and growth of supermassive black holes by comparing and contrasting heavy seed and light seed models?

Pratham Aggarwal[1]★ and Matthew T. Scoggins[2]
[1]*Sidhhartha Public School, Delhi, 110081*
[2]*Department of Astronomy, Columbia University, New York, NY, 10027*

5 June 2023

ABSTRACT
The formation and growth of supermassive black holes (SMBHs) in the early universe is a topic of significant interest in astrophysics. Observational data from high-redshift quasars suggest the existence of SMBHs with masses exceeding $10^9 M_\odot$, posing challenges to understand their formation mechanisms. Different scenarios for the initial seeds of SMBHs, such as heavy seeds and light seeds, are being explored. In this paper, we investigate the insights that can be gained by comparing and contrasting heavy seed and light seed models for the formation and growth of SMBHs. We discuss various formation scenarios for the seeds of SMBHs, including the merging of smaller black holes, the influence of Lyman-Werner background fluctuations, and the conditions in high-redshift quasar host progenitors. We highlight the advantages and disadvantages of heavy seed and light seed models, and their implications for the assembly mechanisms of SMBHs. We also discuss the potential of detecting gravitational waves from SMBH mergers and future prospects for studying the formation and growth of SMBHs. Overall, comparing and contrasting heavy seed and light seed models can provide valuable insights into the formation and growth of SMBHs and shed light on the nature of these enigmatic objects in the early universe.

Key words: quasars: general – galaxies: active – stars: variables: others

1 INTRODUCTION

1.1 Background

Observational data from high-redshift quasars, with redshifts $z \gtrsim 6$, corresponding to an age of the universe of about 0.917 Gyrs ($\sim$ 6.64% of the age of the universe), suggest the existence of quasars with masses exceeding $\geq 10^9 M_\odot$ (for recent reviews, see Fan et al. 2006; Mortlock et al. 2011; Tang et al. 2019 (e.g. SDSS J010013.02+280225.8, a hyperluminous quasar located near the border of the constellations Pisces and Andromeda, with a mass of $\sim 10^{10} M_\odot$ at $z \approx 6.3$, as reported by Wu et al. 2015.) SMBH poses a significant challenge for theories explaining the formation and growth of black holes. According to current understanding, black holes are believed to form as the end result of massive stars. Specifically, black holes that originate from the first generation of massive stars, known as Population III (PopIII) stars, are expected to have initial seed masses that are similar to their final stellar masses (as suggested by studies such as Woosley et al. 2002). However, it is expected that these PopIII remnant black holes are initially starving for accretion material (as indicated by previous studies conducted by Whalen et al. 2004; O'Shea et al. 2005; Wang et al. 2006; Johnson & Bromm 2007; Milosavljević et al. 2009; Alvarez et al. 2009; Jeon et al. 2012). A more recent study by Smith et al. 2018 used a sample of approximately 15,000 PopIII remnant black holes from the `Renaissance` simulation suite (Xu et al. 2013; Chen et al. 2014; O'Shea et al. 2015) to investigate this issue. Their research found no significant evidence of substantial accretion onto these remnant black holes. The study observed that PopIII remnants increased their mass by at most 10% over several hundred million years [1].To explain the growth of black holes beyond the Eddington limit, the super-Eddington model can be analyzed.

1.2 Literature Review

Different scenarios have been proposed for the formation of the first massive black holes (MBHs) in the universe, including the merging of smaller black holes that can lead to the formation of massive black holes with up to $10^9 M_\odot$. Some larger, metal-poor galaxies

★ E-mail: prathamaggarwal7586@gmail.com

[1] It is worth noting, however, that this study focused solely on post-processing analysis and did not account for the potential impact of dynamical friction, which could have influenced the accretion rates.

provide conditions conducive to the rapid formation and growth of "massive seed" black holes through gas accretion and mergers in dense stellar clusters. Detecting the gravitational waves emitted by these mergers using future gravitational wave observatories could be a method to confirm these findings (for recent reviews Inayoshi et al. 2020).Another Possible scenario in which Population III (Pop III) stellar remnants, referred to as "*light seed*s" could serve as the progenitors of supermassive black holes (SMBHs). These Pop III stars are anticipated to form at a redshift of $\sim$ 20-30 within the first collapsed structures, known as *minihalos*. These minihalos are characterized by virial temperatures $T_{vir} < 10^4 K$. The collapse of primordial gas is primarily driven by the cooling effects of molecular hydrogen (e.g., Omukai & Nishi 1998; Omukai et al. 2010). Both hydrodynamical models assuming spherical symmetry and those starting from cosmological initial conditions have shown remarkable agreement in describing the early collapse phase and the formation of the central hydrostatic core (e.g., Yoshida et al. 2008). However, uncertainties still remain regarding the evolution of the post-collapse phase, which involves disk fragmentation, protostellar evolution, and the effects of radiative feedback (e.g., Omukai & Palla 2003; Hosokawa et al. 2011; Greif 2015; Bromm 2013).

An alternative pathway known as the "heavy seed" scenario proposes the existence of black hole seeds with initial masses ranging from approximately $10^4 - 10^6 M_\odot$. One extensively studied version of this pathway is called the direct-collapse black hole (DCBH) scenario. In this scenario, a high accretion rate onto protostars enables the formation of a short-lived supermassive star (SMS), which eventually leads to the formation of a black hole seed with a mass of about $10^4 - 10^6 M_\odot$. Numerous studies have investigated the formation of DCBHs (e.g. Omukai 2001; Bromm & Loeb 2003; Wise et al. 2008; Regan & Haehnelt 2009; Shang et al. 2010; Hosokawa et al. 2012; Latif et al. 2013; Inayoshi et al. 2014; Regan et al. 2014; Becerra et al. 2015; Chon et al. 2016; Latif et al. 2016; Becerra et al. 2018; Wise et al. 2019; Maio et al. 2019; Scoggins et al. 2023)

Other studies suggest that intermediate-mass black holes (IMBH) may play a crucial role in the formation of supermassive black holes .The model suggests that very massive stars, up to $10^4 M_\odot$, can form in early dark matter halos.These stars are exceptionally bright and eventually undergo gravitational collapse, forming intermediate-mass black holes (IMBHs).The accretion of gas and dark matter plays a significant role in the formation of IMBHs. The IMBHs formed through this mechanism could have served as seeds for the formation of supermassive black holes in the early universe.(Umeda et al. 2009)

The influence of Lyman-Werner background fluctuations on the formation of SMBHs has been proposed as a possible explanation, highlighting the role of close halo pairs in facilitating the rapid accretion of gas onto black holes. These fluctuations could significantly impact the formation and growth of SMBHs, with close halo pairs playing a critical role in their formation.The early generation of stars and black holes created a Lyman-Werner background (LWB) at high redshifts before reionization.While the LWB is generally uniform, variations are expected due to the discrete nature and spatial clustering of the sources.The model accounts for the clustering of dark matter halos, Poisson fluctuations in the number of corresponding star-forming galaxies, and scatter in Lyman-Werner luminosity produced by halos of a given mass.Over 99% of dark matter halos are illuminated by a Lyman-Werner flux within a factor of 2 of the global mean value.A small fraction of dark matter halos with $T_{vir} > 10^4 K$ have a close luminous neighbor within a distance of less than $10 kpc$.The presence of close luminous neighbor pairs could play a role in the formation of supermassive black holes.(Dijkstra et al. 2008)

Another pathway is Super-Eddington accretion a scenario that may explain the rapid assembly of supermassive black holes within the first billion years of the Universe. This critical regime is associated with radiatively inefficient accretion and accompanied by powerful outflows in the form of winds.Super-Eddington accretion onto stellar-mass black holes is one possible model for ultraluminous X-ray sources (ULXs).(Massonneau et al. 2022)

1.3 Significance of the study

Studying the formation and growth of supermassive black holes (SMBHs) in the early universe is of great importance as it can provide insights into the evolution of galaxies and the structure of the cosmos. Two popular models for SMBH formation are the heavy seed and *light seed* models. Comparing and contrasting these two models can help us better understand the formation and growth of SMBHs.By examining the Mass distribution of SMBHs over redshift, we can test these predictions and determine which model is more consistent with observations.Furthermore, understanding the formation of SMBHs can also provide insights into the formation of the first stars in the universe.

1.4 Research Objective

Models attempt to explain the mechanisms responsible for the observed properties of SMBHs, such as their masses and growth rates.The existence of SMBHs with masses exceeding 10^9 $M_\odot$ at high-redshift quasars has been observed Different theoretical models, such as Eddington and Super Eddington models, have been explored to explain these phenomena.By comparing and contrasting these different models,research aims to elucidate the physical processes that govern SMBH formation and growth. The findings of this study are expected to provide valuable insights into the mechanisms underlying SMBH formation and growth, and may have implications for our understanding of the early universe and its evolution. The results of this research may also contribute to the development of more accurate theoretical models for SMBH formation and growth, and may help refine our understanding of the role of SMBHs in shaping the structure and properties of galaxies and the larger-scale cosmic web.

1.5 Organization of the Paper

The rest of this paper is organized as follows. In § 2, we introduce the halos used in the study and discuss two growth rates: Eddington and Super Eddington accretion. We also discuss why the concept of capped Eddington growth is impractical. We mention the values used in simulations. Additionally, we introduce the data used in the study to help draw conclusions. In § 3, we present our results for black hole mass ($M_{\rm bh}/M_\odot$). We compare our value of $M_{\rm bh}/M_\odot$ to the value expected in observational data. We also consider other probes which would distinguish heavy-seed *vs.* light-seed pathways. In § 4 we discuss the caveats of the method used in study.Finally, we summarize our findings and offer our conclusions in § 5. Our analysis and data used in this work assume the following cosmological parameters: $\Omega_\Lambda = 0.734$.$\Omega_m = 0.266$, $\Omega_b = 0.049$, and $h = 0.71$.

2 METHODS

The dataset used for analysis in this study is data compiled in Inayoshi et al. 2020, which consists of a comprehensive list of 203 quasars.The dataset includes properties of the quasars, such as redshift and Mass.Masses are obtained from the rest-frame UV magnitude M_{1450} as: Mass = $10^{-[(M_{1450}+3.459)/2.5]}$, which yields, on average, the published virial mass estimates for those quasars for which virial masses are available. In our analysis, we specifically consider two models: the "heavy seed" model with seed masses ranging from $10^4 - 10^6$ $M_\odot$ and the "*light seed*" model with seed masses ranging from $10^2 - 10$ $M_\odot$.During the analysis, we make the assumption that the growth rate of these seeds follows the Eddington rate, Additionally, we also explore the possibility of Super-Eddington growth, which refers to an accretion rate exceeding the Eddington limit.

2.1 Calculating black hole mass

Eddington Accretion

The Eddington luminosity (L_{edd}) represents the maximum luminosity that a black hole can achieve due to the balance between the gravitational force and the radiation pressure.

$$L_{\rm edd} \equiv \frac{4\pi c G \mu m_{\rm p} M_{\rm bh}}{\sigma_{\rm T}} = \epsilon c^2 \dot{M}_{\rm bh}, \tag{1}$$

with speed of light c, gravitational constant G, mean molecular weight μ ($\mu \sim 0.6$ for primordial ionized gas), proton mass $m_{\rm p}$, Thomson cross section $\sigma_{\rm T}$, and radiative efficiency ϵ. This leads to a black hole mass given by $M_{\rm bh}(t) = M_{\rm i} \exp(t/\tau_{\rm fold})$ with e-folding time $\tau_{\rm fold} = (\sigma_{\rm T} c \epsilon)/(4\pi\mu G m_{\rm p}) \approx 450\epsilon$ Myr. Now we analyze two different approaches to analyze the growth of SMBH: *light seed* and *heavy seed* models.

2.1.1 *Light Seed Model*

Quasars, as indicated by observational data, have been found to grow to masses of approximately $10^9 M_\odot$ at a redshift of $z \approx 6$. Here it is believed that these quasars start from smaller "*light seed*".To account for the observed growth in mass within a reasonable timescale, the efolding time ($\tau_{\rm fold}$) becomes crucial.Considering Eq. 1, a smaller value for $\tau_{\rm fold}$ would result in a more rapid growth, allowing the quasar to reach the observed mass within an appropriate timeframe. In the analysis, three possible values for $\tau_{\rm fold}$ are considered, $\tau_{\rm fold} \in \{20, 40, 80\}$ Myr.We explore an initial seed mass of $M_{\rm i} \in \{100, 50, 10\}$ $M_\odot$to investigate different growth scenarios and their implications.Growth is shown in Fig. 3.

2.1.2 *Heavy Seed Model*

Similarly, as discussed in Section § 2.1.1,Since in this model quasars start from heavier state we consider $\tau_{\rm fold} \in \{20, 40, 80\}$ Myr to ensure appropriate growth of the quasar.For our purposes, we explore a range of parameters. Initial seed masses in the `Renaissance` simulation are estimated to fall within the range $10^4 M_\odot \leq M_{\rm bh} \leq 10^6 M_\odot$, in agreement with the expected seed mass for the DCBH formation pathway, so we explore an initial seed mass of $M_{\rm i} \in \{10^4, 10^5, 10^6\}$ $M_\odot$.Growth is shown in Fig. 2.

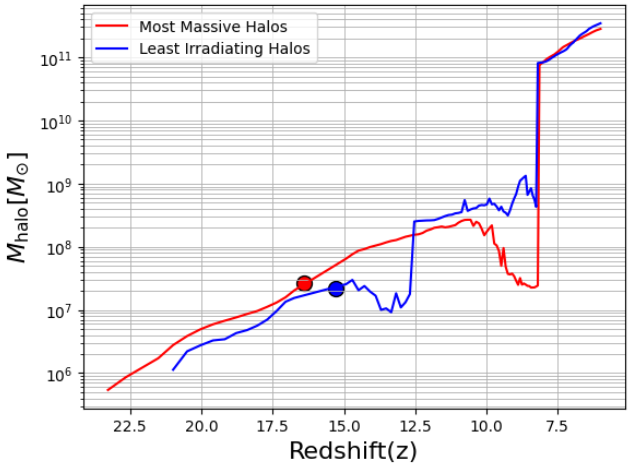

Figure 1. The total mass of two target haloes, MMH and LWH, changes over time, specifically as a function of redshift. The formation of the black hole within each halo is denoted by dots on the graph. MMH's black hole forms at a redshift of $z = 16.4$, while LWH's black hole forms slightly later at $z = 15.3$.MMH undergoes tidal stripping between redshifts $z = 11 - 8$ as it moves through a more massive halo known as the "Superhost" halo. Eventually, at around redshift $z \sim 8$, MMH completely merges with the Superhost halo. On the other hand, LWH also experiences a smaller tidal stripping event near redshift $z \sim 14$ before eventually merging completely with its own Superhost halo at redshift $z \sim 8$. It's important to note that the Superhost haloes that MMH and LWH merge with are distinct and separated by a distance greater than 2 Mpc at $z \geq 7$

2.2 Constraining the growth

Fig. 2 and 3 convey that mass of quasar is growing massive and also in such a short span ~ 0.8Gyr $M_\odot$. According to King 2015, SMBHs cannot grow larger than $M_{\rm max}$ because $M_{bh} > M_{\rm max}$ makes disk formation impossible.

$$M_{\rm max} = 5 \times 10^{10} M_\odot \alpha^{7/3} \eta_{0.1}^{4/13} \left(\frac{L}{L_{\rm Edd}}\right)^{-4/13} f_5^{-27/26} \tag{2}$$

represents the maximum mass ($M_{\rm max}$) that a black hole can attain. The constant factor $5 \times 10^{10} M_\odot$ denotes the scale of the maximum mass in terms of solar masses.The term $\alpha^{7/3}$ relates to the efficiency of accretion, where α represents the dimensionless viscosity parameter. The term $\eta_{0.1}^{4/13}$ relates to the radiative efficiency (η) of the accretion process, with $\eta_{0.1}$ being the efficiency normalized to 0.1, $f_5^{-27/26}$ indicates additional factors that can influence the maximum mass, denoted by the variable f.All in all variables represented are fractions therefore black holes will not grow ($\{10^{26} M_\odot, 10^{15} M_\odot, 10^{11} M_\odot\}$)to such a massive amount,so we constrain the growth when the mass of the black hole exceeds a prescribed fraction of the baryonic matter in the halo, capping $M_{\rm bh} \leq f_{\rm bh} M_{\rm halo} \Omega_{\rm b}/\Omega_{\rm m}$ with $f_{\rm bh} \in \{0.05, 0.1, 0.2, 0.5\}$ We use the stellar halo mass used in Scoggins et al. 2023. Fig.1 show the halos used in study.

We now proceed to examine the black holes that have undergone growth, as illustrated in Fig. 4 and 5, specifically focusing on high redshift ($z \leq 7$). To provide a basis for comparison, we refer to the observed quasars dataset. By analyzing the black holes depicted in Figures 4 and 5 within the context of high redshift ($z \leq 7$), we aim to draw meaningful comparisons between the simulated black holes and the observed quasars.By plotting the discrete data

and simulated results we compare and dig valuable insights.This comparative analysis will shed light on the growth patterns and properties of black holes in the early universe.

2.3 Exploring alternate growth rate: beyond limits

The observed masses of SMBHs in quasars also pose intriguing challenges for their formation mechanisms. The standard model of black hole growth through accretion of matter, limited by the Eddington luminosity, is unlikely to account for the observed masses. Therefore, alternative scenarios for the initial seeds of SMBHs have been investigated.

When a quasar surpasses the Eddington limit, it signifies that the energy generated by the accretion process overwhelms the gravitational force acting on the matter falling into the black hole's accretion disk. This phenomenon typically occurs when there is an exceptionally high rate of matter infall into the black hole. As matter falls into the accretion disk, it forms a swirling disk of superheated gas and dust surrounding the black hole. The gravitational pull of the black hole attracts the matter inward, leading to a release of gravitational potential energy. This energy is converted into heat, causing the accretion disk to emit intense radiation across a wide range of wavelengths, including X-rays and ultraviolet light.However, there is a limit to how much energy can be released from the accretion process ,The Eddington limit , Beyond this limit, the radiation pressure dominates, and it inhibits further accretion by pushing the infalling matter away. (Jiang et al. 2014; Sądowski et al. 2014; Inayoshi et al. 2016; Toyouchi et al. 2021) provide a simple prescription for the rate of black hole growth $\dot{M}_{\rm bh}$ (see their Eq.1) which is simplified in Scoggins et al. 2023

$$\dot{M}_{\rm bh} = \dot{M}_0^{1-p} \left(\frac{3}{5}\dot{M}_{\rm Edd}\right)^p \quad \text{if} \quad \frac{3}{5}\dot{M}_{\rm Edd} \leq \dot{M}_0 \tag{3}$$

and $\dot{M}_{\rm bh} = \dot{M}_0$ otherwise. We approximate gas supply as constant,

$$\dot{M}_0 \approx \mathscr{F}\frac{\Omega_{\rm b}}{\Omega_{\rm m}}\frac{M_{\rm halo}(t) - M_{\rm halo}(t_0)}{t - t_0} \tag{4}$$

for $\mathscr{F} \sim 0.1$. This allows us to solve for the mass of the black hole,

$$M_{\rm bh}(t) = \dot{M}_0 \left(\frac{3}{5\tau_{\rm fold}}\right)^{\frac{p}{1-p}} [(t-t_0)(1-p)]^{\frac{1}{1-p}} + M_{\rm bh}(t_0) \tag{5}$$

for a period from t_0 to t where $(3/5)\dot{M}_{\rm Edd} \leq \dot{M}_0$, otherwise $M_{\rm bh}(t) = \dot{M}_0(t - t_0) + M_{\rm bh}(t_0)$.Using $p = 0.6$ we plot the growth of blackhole which is shown in Fig.7 for heavy seed and Fig.8 for light seed scenario.

3 RESULTS AND DISCUSSION

3.1 Discussing for Eddington growth

3.1.1 Contrasting growth factors

In the *light seed* model, the growth of black holes is observed to be monotonically increasing. For a $\tau_{\rm fold}$ value of 20 Myr, the growth initially follows a linear trend. However, as the e-folding time decreases, the growth becomes more rapid and exponential. The *light seed* model exhibits overall efficient and continuous growth of black holes.

On the other hand, in the heavy seed model, fluctuations and variations are encountered during the growth of black holes. These fluctuations arise due to the interactions and mergers between some heavier halo and Lyman Werner halo (LWHs). Unlike the *light seed* model, the heavy seed model experiences more frequent saturations, where the growth temporarily plateaus.It is important to note that the growth of black holes in both models is influenced by the e-folding time ($\tau_{\rm fold}$). The *light seed* model, with its shorter $\tau_{\rm fold}$, follows an overall exponential growth trend, resulting in a more efficient and continuous increase in black hole mass. In contrast, the heavy seed model deviates from exponential growth due to the fluctuations and sudden jumps, which are more prominent with longer $\tau_{\rm fold}$ values.Overall, the comparison between the *light seed* and heavy seed models highlights the impact of initial conditions and e-folding time on the growth of black holes and the behavior of halos. The *light seed* model demonstrates a more consistent and efficient growth, while the heavy seed model encounters fluctuations and reaches saturations more frequently, leading to a less smooth and more discontinuous growth pattern.

3.1.2 Growth of LWH vs MMH

In Figure 4 $\tau_{\rm fold} \in \{20, 40\}$Myr, the growth of the Massive Main Halo (MMH) is observed to be initially smooth and steadily increasing. However, it eventually reaches a point where its growth becomes constant for a certain interval. This behavior can be attributed to the MMH starting to accrete into a heavier halo, which is evident when the MMH reaches the knee mass On the other hand, the Lyman Werner Halo (LWH) in Figure 4 exhibits fluctuations due to resistive agents. Unlike the MMH, the LWH does not experience a constant growth phase but rather shows varying levels of accretion. Nevertheless, similar to the MMH, the LWH also demonstrates a linear growth trend with a higher slope, indicating an interaction between the LWH and a heavier halo. Eventually, both the MMH and LWH merge into their respective heavier halos. However if we consider $\tau_{\rm fold} = 80$Myr growth is exponential and less efficient. On the other hand Fig.5 for light seed model $\tau_{\rm fold} = 20$Myr we see that similar characteristics are observed between MMH and LWH as of Heavy seed model. However for $\tau_{\rm fold} \in \{40, 80\}$Myr like heavy seeds $\tau_{\rm fold} \in \{40, 80\}$Myr growth is exponential and efficient for $\tau_{\rm fold} = 40$Myr whereas $\tau_{\rm fold} = 80$Myr will take much more time as compared to other efolding time ($\tau_{\rm fold}$) , in other words is inefficient growth.

3.1.3 Growth of Light seed vs Heavy seed

In the analysis of Fig.6, it is observed that for a folding timescale of $\tau_{\rm fold} = 20$ Myr, the model tends to overestimate the growth of the quasar. This suggests that the quasar is more efficient in its accretion process and reaches the mass of a supermassive black hole (SMBH) at an earlier stage than predicted by the model. This scenario indicates that there is a subset of quasars with rapid growth, which is consistent with the observed heavy quasars with masses $\geq 10^9$ M$\odot$ in the high redshift range $z \geq 7$. This positive aspect is clearly depicted in Column 1 of Fig.6.On the other hand, if we consider a folding timescale of $\tau_{\rm fold} = 80$ Myr, the light seed model is not adequate in predicting the observed quasars, as shown in Column 3 of Fig.6. The light seed model underestimates the growth of the quasars, resulting in them being less massive compared to the observed quasars in the redshift range $z \in (6.4, 6)$. This discrepancy suggests that the light seed model may not capture the dynamics and behaviors of quasars with slower growth rates accurately.Overall, the analysis highlights the importance of considering different efolding timescales in understanding the growth of quasars. The observed overestimation of quasar growth for a folding timescale of $\tau_{\rm fold} = 20$

Myr provides insights into the behavior of heavy observed quasars, particularly those with masses $\geq 10^9$ $M_\odot$. However, the light seed model may not be sufficient for predicting the growth of quasars in the redshift range $z \in (6.4, 6)$ accurately. Further investigations and refinements of the model may be necessary to improve its agreement with observational data.

The analysis of observed data within the redshift range of $z \in (7.2, 6.4)$, using a folding timescale of $\tau_{\rm fold} = 40$ Myr, reveals interesting insights about the two seed models (light and heavy) in different mass intervals.When considering the mass range $M_{bh} \in (10^8, 10^9)$, it becomes evident that the heavy seed model provides a more accurate representation compared to the light seed model. This indicates that for quasars with masses in this range, the formation and growth processes are better described by a scenario where black holes start with a significant seed mass. The heavy seed model proves to be more appropriate in capturing the observed characteristics of quasars within this mass interval at the given redshifts.However, extending the analysis to higher redshifts ($z \geq 6.4$) introduces a shift in the behavior of the seed models. In this regime, the heavy seed model continues to be a suitable choice for the heavier observed quasars with masses falling within $M_{bh} \in (10^8, 10^9)$. On the other hand, the light seed model emerges as a better fit for the lighter observed quasars, encompassing the mass range $M_{bh} \in (10^7, 10^8)$.This shift in the preferred seed model at higher redshifts implies that the formation and growth mechanisms of quasars might vary depending on the mass range being considered. It suggests that at earlier cosmic times, lighter seed masses are more conducive to explain the observed properties of lower mass quasars, while heavier seed masses are favored for higher mass quasars. This observation highlights the importance of accounting for both redshift and mass intervals when determining the most suitable seed model for a given population of quasars.In summary, the analysis of quasar data within the specified redshift range and using a folding timescale of $\tau_{\rm fold} = 40$ Myr indicates that the heavy seed model is better suited for quasars with masses $M_{bh} \in (10^8, 10^9)$ in the considered mass interval. However, at higher redshifts, the heavy seed model remains appropriate for heavier quasars, while the light seed model proves more accurate for lighter quasars within the mass range $M_{bh} \in (10^7, 10^8)$.

3.1.4 Insepecting and Contrasting via Observation

In Fig. 6 we present additional analyses that provide further insights into the behavior of the system. We specifically investigate the impact of different folding timescales ($\tau_{\rm fold}$) on the growth of the halos. Firstly, when considering a folding timescale of $\tau_{\rm fold} = 30$ Myr, as mentioned earlier, we observe the growth of the MMH and LWH halos and their eventual merging to form a supermassive black hole (SMBH). However, it is crucial to note that the choice of $\tau_{\rm fold}$ has a significant influence on the merging timescale. In this case, a folding timescale of 30 Myr leads to a longer merging process compared to $\tau_{\rm fold} = 5$ Myr and $\tau_{\rm fold} = 20$ Myr.

Additionally, in the heavy seed case, the general trend remains consistent. For $\tau_{\rm fold} = 40$ Myr, we find that the model provides quite accurate estimations for the growth of MMH halos with heavy seeds, particularly when considering the assumed Eddington growth rate. This suggests that adjusting the folding timescale appropriately allows the model to capture the growth dynamics of MMH halos with heavy seeds effectively.

However, when we set $\tau_{\rm fold} = 80$ Myr, we observe that the model tends to underestimate the growth of the halos. Consequently, a folding timescale of 80 Myr is not suitable for capturing the true growth dynamics of the system accurately.

Our findings demonstrate the substantial influence of the folding timescale on the timescale of halo merging. Moreover, in the case of heavy seed halos, setting $\tau_{\rm fold} = 40$ Myr yields more precise estimations when considering the assumed Eddington growth rate. Conversely, caution should be exercised when using a folding timescale of 80 Myr, as it leads to an underestimation of the halo growth.

When considering an Eddington Accretion scenario the Heavy Seed Model emerges as a significant framework.In the Heavy Seed Model, it is proposed that the initial seed black holes, from which SMBHs grow, possess substantial mass. This model aligns with observations suggesting that the early universe contained black holes with masses on the order of thousands to millions of times that of the Sun. The Heavy Seed Model estimates prove to be quite accurate, particularly when the characteristic timescale for the quasar's fading, referred to as the "folding timescale" ($\tau_{\rm fold}$), is around 40 million years (40 Myr).

When $\tau_{\rm fold}$ is approximately 40 Myr, the Heavy Seed Model successfully predicts the properties and behavior of quasars. This timescale reflects the period over which a quasar transitions from a luminous state to a relatively quiescent or "quiet" phase. During this transition, the accretion rate onto the black hole decreases, causing the quasar's luminosity to fade.

Furthermore, the Heavy Seed Model implies that the black hole's growth is fueled by a combination of Eddington-limited accretion and mergers with other black holes. As the black hole accretes matter, it emits intense radiation and displays the characteristic features of a quasar. However, as the accretion rate declines over the folding timescale of 40 Myr, the quasar's activity subsides, leading to a quieter phase.

By considering the Eddington Accretion scenario and incorporating the Heavy Seed Model, scientists can explain the observed properties and behavior of quasars, particularly when $\tau_{\rm fold}$ is approximately 40 Myr. This combination provides a useful framework for understanding the formation and evolution of SMBHs, shedding light on the intricate processes at play in the universe's early stages.(for reference see 6)

3.2 Discussing for super-Eddington growth

In Fig.9 When analyzing the properties of heavy observed quasars with masses around $\sim 10^9 M_\odot$, the existing model proves to be suitable and effective. However, when we shift our focus to studying light observed quasars with masses $\geq 10^9 M_\odot$, it becomes apparent that the current model is inadequate and insufficient for describing their characteristics accurately.The model's applicability for heavy observed quasars, which typically have masses on the order of $10^9 M_\odot$, implies that it successfully captures and explains their behavior. These massive quasars exhibit unique properties due to their significant mass, allowing the current model to adequately account for their dynamics and associated phenomena.However, as we examine the population of lighter observed quasars, those with $\geq 10^9 M_\odot$, the limitations of the existing model become evident. Light quasars often display distinct characteristics and behaviors that deviate from the patterns observed in their heavier counterparts. Consequently, the current model fails to provide a comprehensive understanding of their properties, suggesting the need for an alternative or refined framework to describe these phenomena accurately.

4 EXPLORING LIMITATIONS: UNCOVERING CONSTRAINTS AND CHALLENGES

The Eddington accretion model assumed in study,while valuable for understanding accretion processes, has some limitations. It assumes spherical symmetry, does not take into account non-spherical structures and asymmetries in the accretion flow. Magnetic fields, which are known to affect the accretion dynamics, are not taken into account. The model ignores turbulence and viscosity, which significantly affect the transport of mass and angular momentum. Moreover, it simplifies radiation processes and neglects the complex effects of radiation transfer.(for reviews Abramowicz & Fragile 2013; Tristram & Ganga 2007; Svestka 1972) Each supermassive black hole (SMBH) and its corresponding quasar possess unique properties and characteristics. General conclusions directly cannot be drawn without considering the individuality of each object. Quasars emit radiation with varying wavelengths, ranging from visible to X-rays and radio waves. The rate of material accretion onto the SMBH differs among quasars, affecting their luminosity and observational traits. SMBHs come in a range of masses, impacting the size, brightness, and influence on surrounding galaxies. Quasars exhibit temporal variability patterns, reflecting diverse accretion processes and environments. Interactions with host galaxies further influence quasar behavior. Comprehensive study of a diverse range of objects is essential to comprehend the complexity and diversity of SMBHs and quasars.

5 CONCLUSIONS

Various models have been proposed to explain the formation of supermassive black holes (SMBHs), yet their existence remains largely unknown. In order to gain insights into this phenomenon, we have conducted analyses using different rates of accretion, specifically the Eddington and super-Eddington rates. These rates were then incorporated into the light seed and heavy seed models to predict the expected evolution of quasars, which are highly luminous active galactic nuclei powered by accretion onto SMBHs.However, it is important to acknowledge the limitations of these models, as discussed in § 4. These limitations may include uncertainties in the physical processes involved in the growth of SMBHs, the complexity of the accretion process, and the potential impact of feedback mechanisms on the growth of SMBHs.Taking into account the predicted results obtained from our analyses and comparing them with observational data, we gain valuable insights. By plotting the predicted results alongside the observational data, we make meaningful comparisons regarding the viability of different formation pathways for SMBHs.Upon evaluating the results, we arrive at the conclusion that the heavy seed model provides a more plausible pathway for the formation of SMBHs compared to the light seed model. The heavy seed model suggests that SMBHs are formed through the direct collapse of massive gas clouds or the rapid accretion of pre-existing intermediate-mass black holes. This mechanism allows for the rapid growth of SMBHs from the early stages of the universe.In contrast, the light seed model proposes that SMBHs initially form from the remnants of massive stars through stellar evolution processes. However, this model faces challenges in explaining the rapid growth of SMBHs observed in the early universe, as it requires prolonged periods of accretion.In summary, our analysis and comparison of the predicted results with observational data support the notion that the heavy seed model offers a more favorable pathway for the formation of SMBHs. Nonetheless, further research and observational evidence are required to fully understand the formation mechanisms of these enigmatic objects.

ACKNOWLEDGEMENTS

I would like to express my sincere gratitude to Mr. Scoggins, Research Mentor, for his valuable feedback, insightful discussions, and for providing important halo data necessary for my study. His contributions have greatly enhanced the quality and accuracy of our research.I would also like to acknowledge the assistance of Chloé-Rose, Writing Coach, who provided valuable guidance and support throughout the process of drafting the manuscript. Her expertise and advice were instrumental in improving the clarity and coherence of my work.I also want to thank Tanvika Parlikar, Program Manager, for helping my research conclude smoothly.The plotting library Matplotlib (Hunter 2007) was used to construct the plots in this paper.Additionally, I extend my appreciation to the entire research community for their contributions to the field. Their work and insights have been invaluable in shaping our understanding of the subject matter.

DATA AVAILABILITY

Observational data used in manuscript is the data compiled in Inayoshi et al. 2020 (Supplementary Material).Halo data follows Behroozi et al. 2019 and required modifications is done in Scoggins et al. 2023.The code used during the preparation of this manuscript is available at this github repository

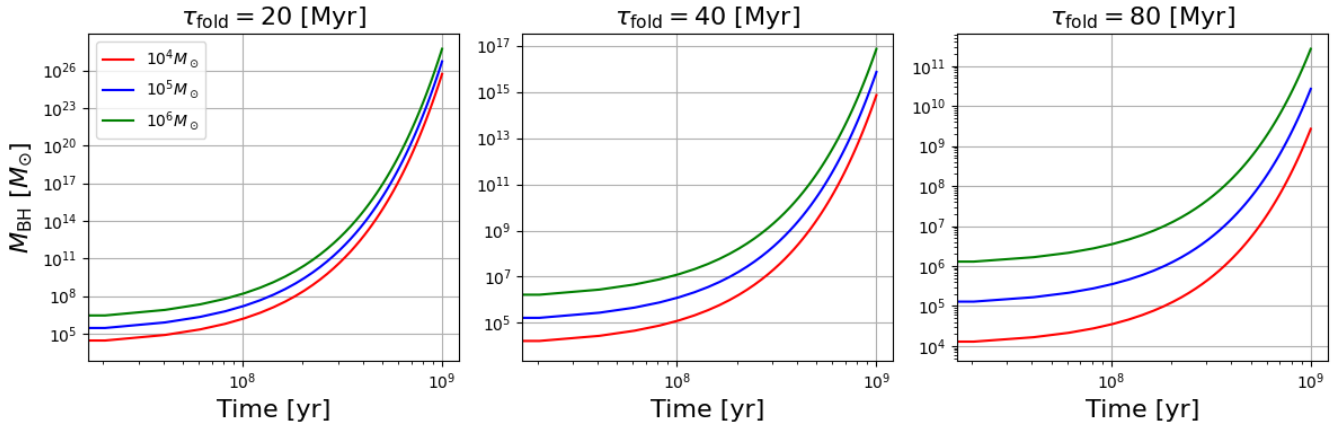

Figure 2. The figure illustrates the growth of Supermassive Black Holes (SMBHs) over time, considering the Eddington limit as the governing rate. The focus of the analysis is on heavy seed SMBHs, which are characterized by initial masses of $M_i = \{10^4, 10^5, 10^6\}M_\odot$ for different efolding time $\tau_{\rm fold} \in \{20, 40, 80\}$Myr.The vertical axis represents the mass of the SMBH in solar mass, while the horizontal axis corresponds to time in yr. The growth of SMBHs is depicted as an exponential curve, indicating the increasing mass of the quasars.However quasars grow unrealistically massive reaching $\{10^{26}, 10^{17}, 10^{11}\}M_\odot$, which indicates the requirement of constraining the growth.

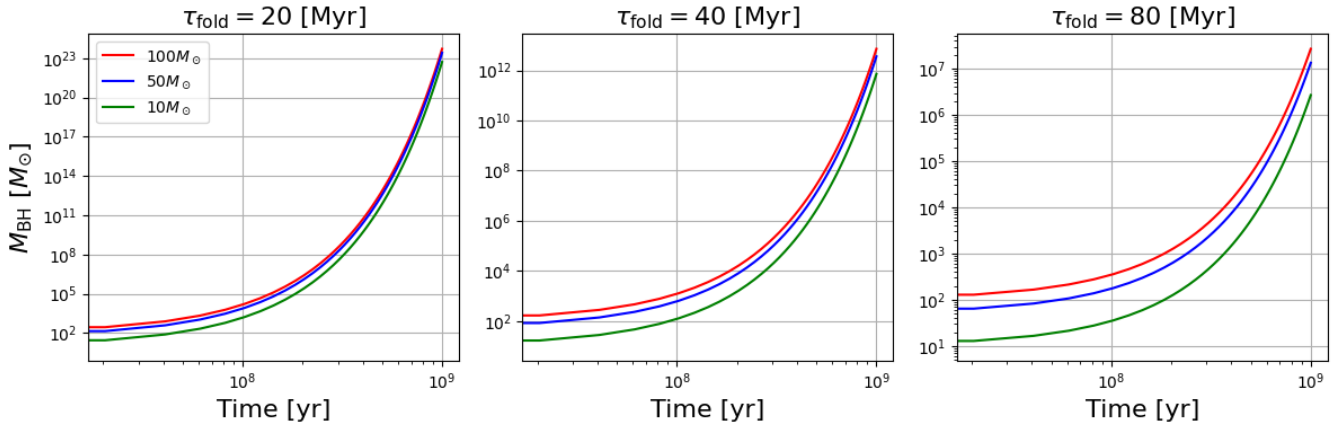

Figure 3. The figure illustrates the growth of Supermassive Black Holes (SMBHs) over time, considering the Eddington limit as the governing rate. The focus of the analysis is on heavy seed SMBHs, which are characterized by initial masses of $M_i = \{10^2, 50, 10\}M_\odot$ for different efolding time $\tau_{\rm fold} \in \{20, 40, 80\}$Myr.The vertical axis represents the mass of the SMBH in solar mass, while the horizontal axis corresponds to time in yr. The growth of SMBHs is depicted as an exponential curve, indicating the increasing mass of the quasars.However quasars grow unrealistically massive reaching $10^{23}M_\odot$, which indicates the requirement of constraining the growth.

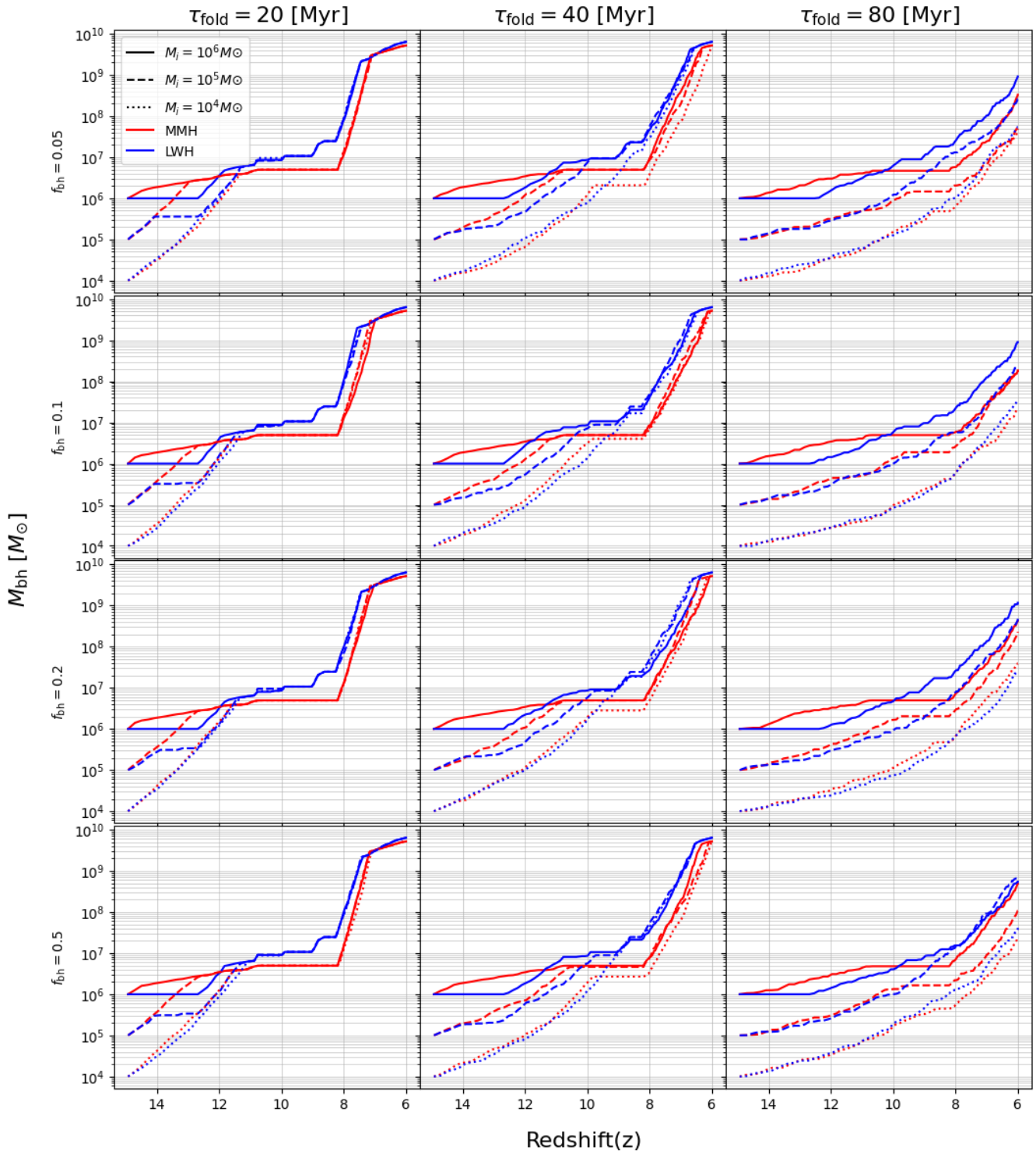

Figure 4. The figure illustrates the growth of a quasar as a function of the Eddington accretion rate (M_{bh}) in solar mass units. We account our calculations for heavy seed $M_{bh} \in \{10^6, 10^5, 10^4\} M_\odot$ Unlike the growth depicted in Figure 2, the growth of this particular quasar is quenched. To account for this quenching effect, we employ an approximation stating that quasars cannot accrete gas exceeding a fraction of the baryonic mass available in the halo. Specifically, we have the condition $M_{bh} \leq f_{bh} M_{halo} \Omega_b / \Omega_m$, where $f_{bh} \in \{0.05, 0.1, 0.2, 0.5\}$.Examining the behavior of the two halos, MMH (Most Massive Halo) and LWH (Lyman Werner Halo), we observe distinct patterns. for tau_{fold} = 20Myr The MMH remains relatively smooth and becomes constant ($z \in [12, 8]$) until it merges with a more massive halo within the redshift around 8. This merging event indicates that the MMH combines with a significantly heavier halo, potentially influencing the quasar growth within that timeframe.In contrast, the LWH experiences fluctuations before eventually merging with a heavy halo around redshift 11. Subsequently, at a later stage characterized by around redshift 8, the LWH merges with a massive halo. These merging events and the associated fluctuations likely play a role in shaping the growth and quenching behavior of the quasar residing within the LWH.

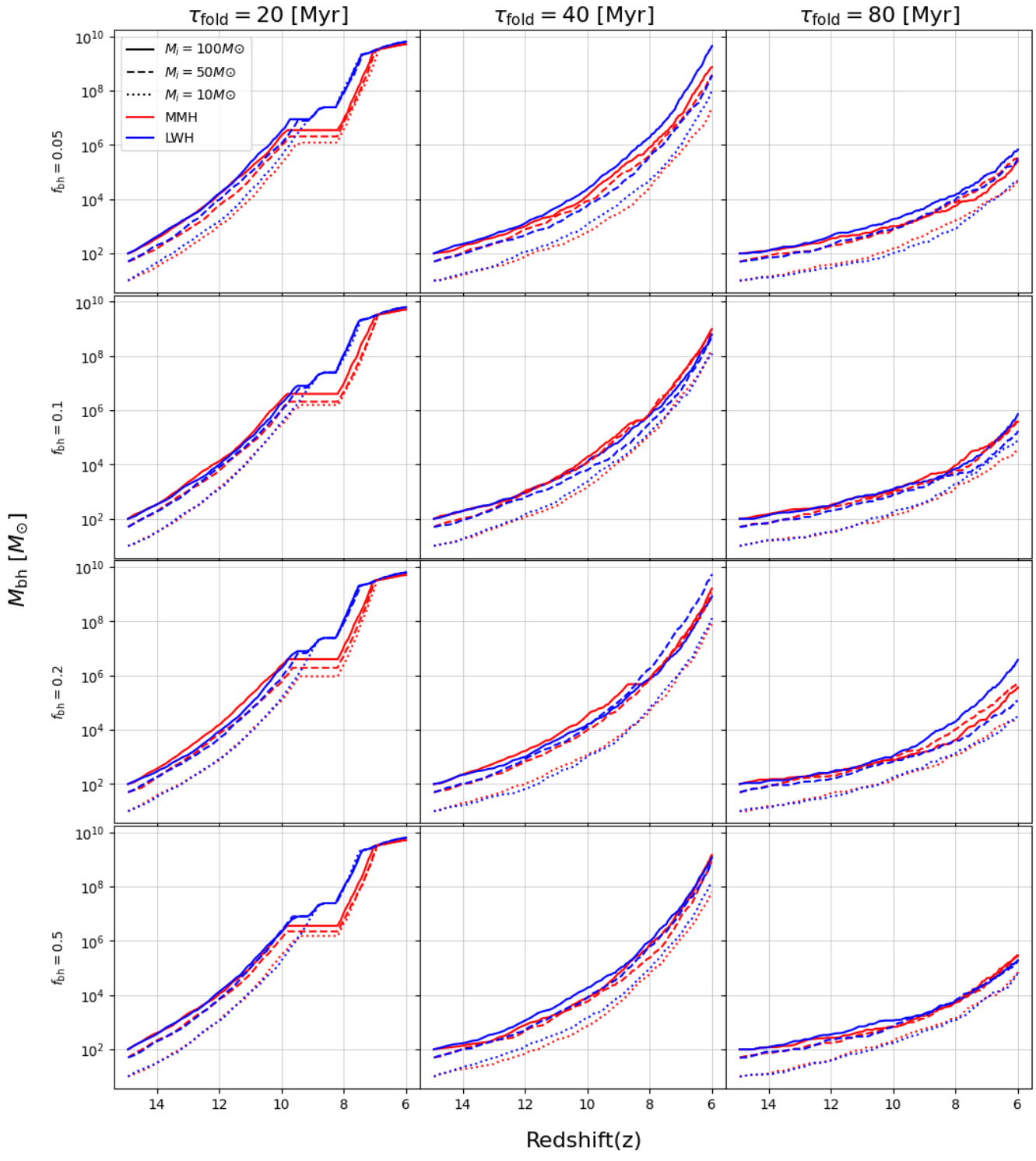

Figure 5. The figure shows the growth of a quasar as the Eddington accretion rate (Mbh) varies, considering light seed black holes with initial masses of Mbh $\in \{100, 50, 10\}M_\odot$. In contrast to the typical growth pattern, this quasar's growth is quenched by a condition that limits the accretion of gas based on the available baryonic mass in the halo.Two types of halos are examined: the Most Massive Halo (MMH) and the Lyman Werner Halo (LWH). The MMH shows relatively smooth and constant growth between redshifts 12 and 8, but later merges with a heavier halo around redshift 8. The merging event affects the quasar's growth within that timeframe, especially when the quasar's folding timescale ($\tau_{\rm fold}$) is 20 Myr. When $\tau_{\rm fold} \in \{40, 80\}$Myr, the MMH exhibits smoother growth similar to the uncapped version.In contrast, the LWH experiences fluctuations in its growth and eventually merges with a heavy halo around redshift 11. Subsequently, around redshift 8, the LWH merges with a massive halo, influencing the quasar's growth. These merging events and fluctuations significantly shape the growth and quenching behavior of the quasar within the LWH. The choice of $\tau_{\rm fold} \in \{40, 80\}$Myr.

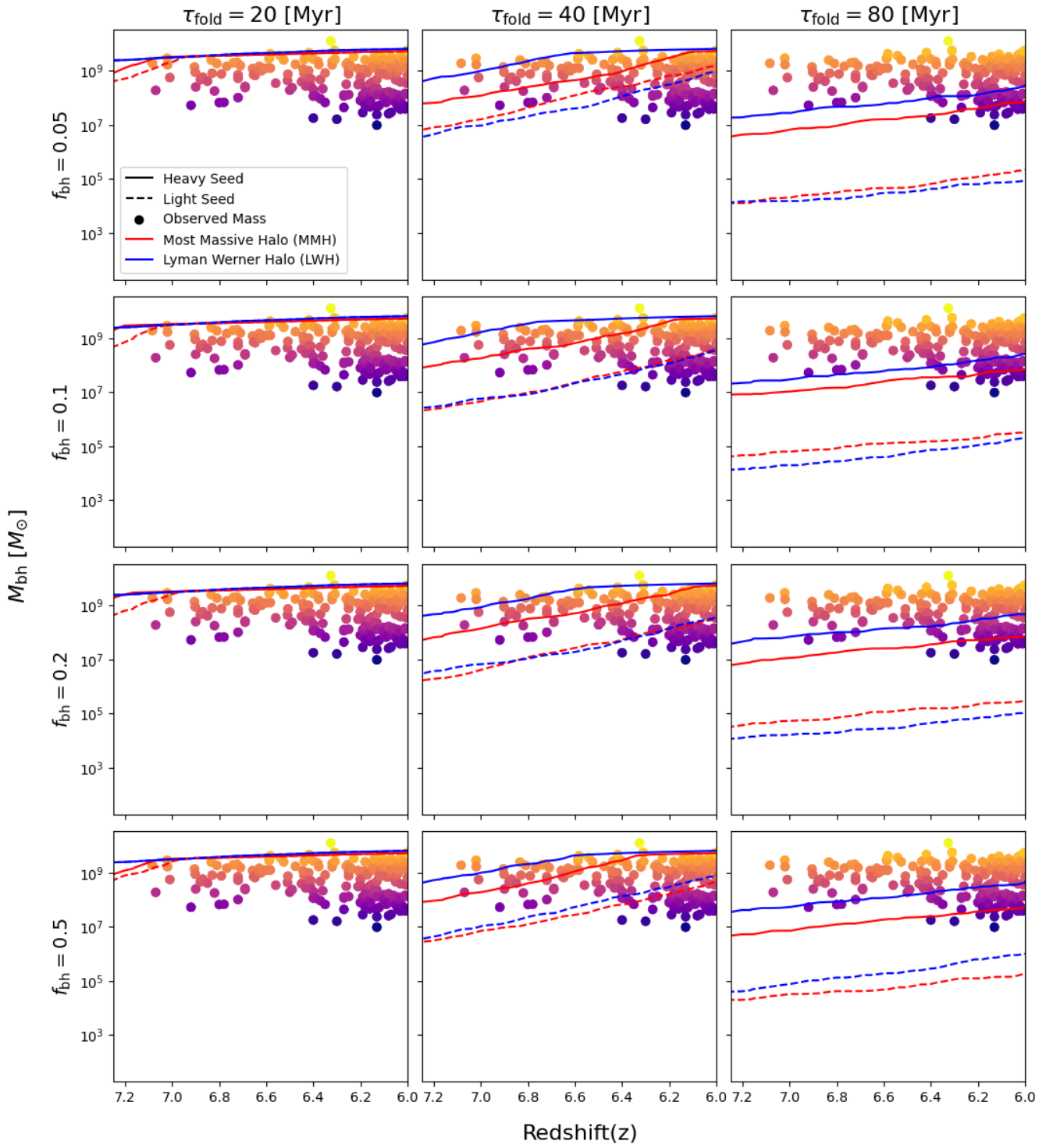

Figure 6. This figure illustrates the growth of supermassive black holes (SMBHs) with heavy and light seed masses over a redshift range of $z \in [7.1, 6]$.Growth rate is assumed to be Eddington rate .The heavy seed has a mass of $M_{bh} = 10^5$ M$\odot$, while the light seed has a mass of 50 M$\odot$. The growth is examined for various fractions of black hole seeds, f_{bh}, which are set to $\{0.05, 0.1, 0.2, 0.5\}$, and different folding timescales, τ_{fold}, which are chosen from $\{20, 40, 80\}$ Myr.The growth of SMBHs in solar mass units is compared against the observed quasars compiled in Inayoshi et al. 2020.We gain valuable insights into the assembly of these massive cosmic objects.

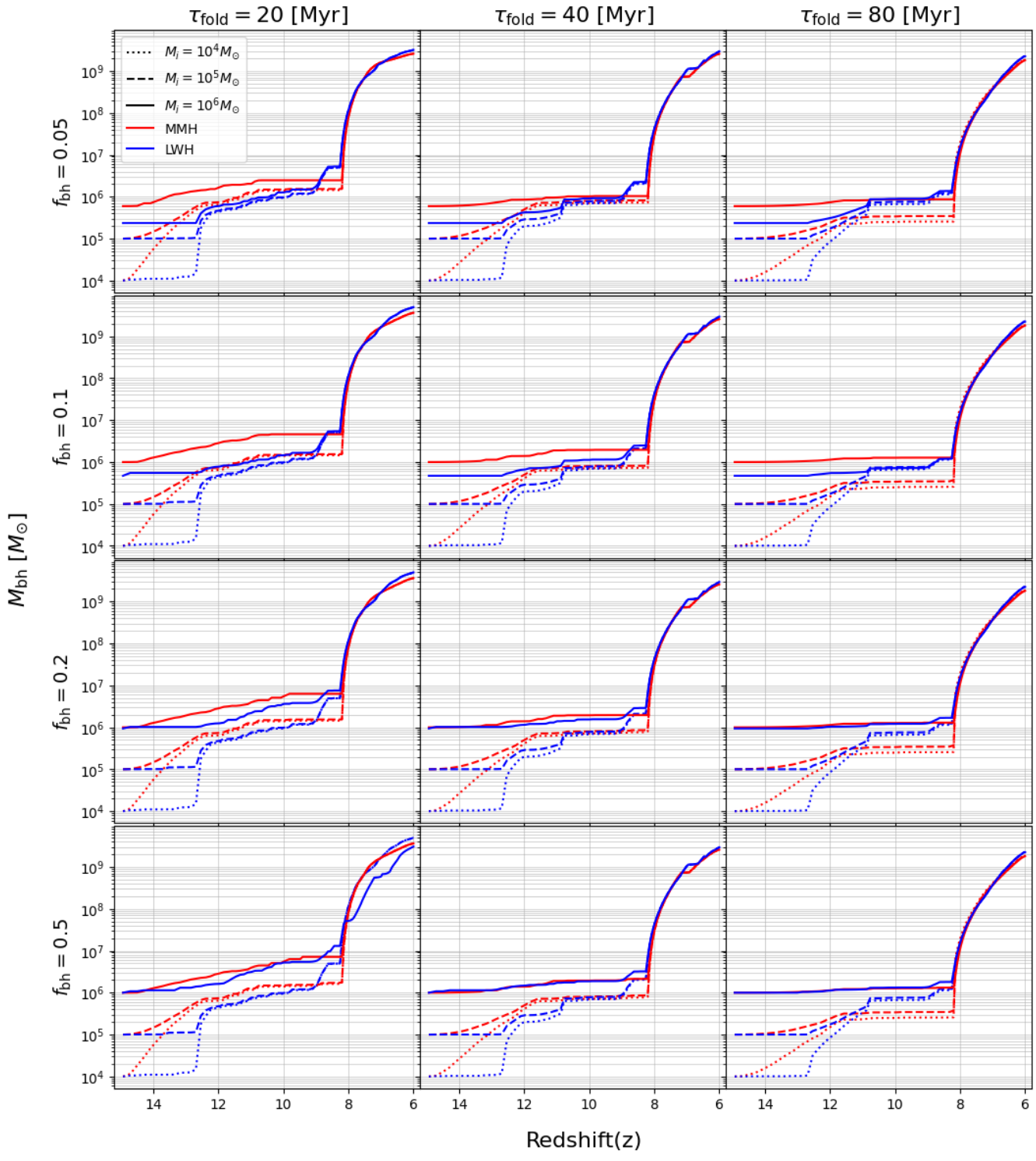

Figure 7. Figure shows the growth of SMBH according to super-Eddington rate for different masses specifically heavy seed ($\{10^4, 10^5, 10^6\}$M$_\odot$)The black hole growth is determined by the large-scale mass inflow rate $\dot{M}_0$, where $\dot{M}_{\rm bh} = \dot{M}_0^{0.4} \left[(3/5)\dot{M}_{\rm Edd}\right]^{0.6}$ if $\dot{M}_0 \geq (3/5)\dot{M}_{\rm Edd}$ (accounting for suppression due to outflows produced by trapped radiation), and $\dot{M}_{\rm bh} = \dot{M}_0$ otherwise.

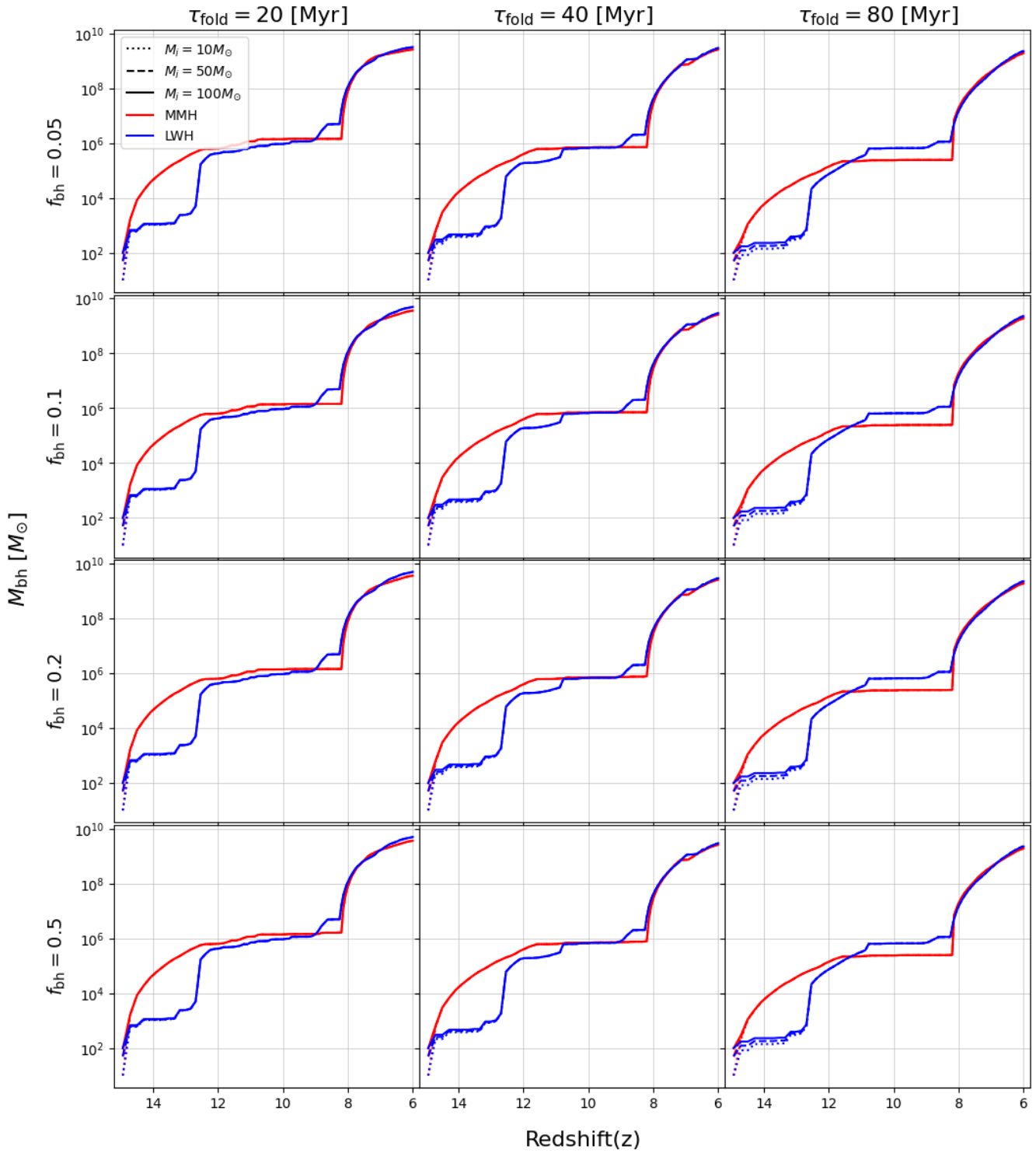

Figure 8. Figure shows the growth of SMBH according to super-Eddington rate for different masses specifically light seed ($\{100, 50, 10\}M_\odot$)The black hole growth is determined by the large-scale mass inflow rate $\dot{M}_0$, where $\dot{M}_{bh} = \dot{M}_0^{0.4}\left[(3/5)\dot{M}_{Edd}\right]^{0.6}$ if $\dot{M}_0 \geq (3/5)\dot{M}_{Edd}$ (accounting for suppression due to outflows produced by trapped radiation), and $\dot{M}_{bh} = \dot{M}_0$ otherwise.

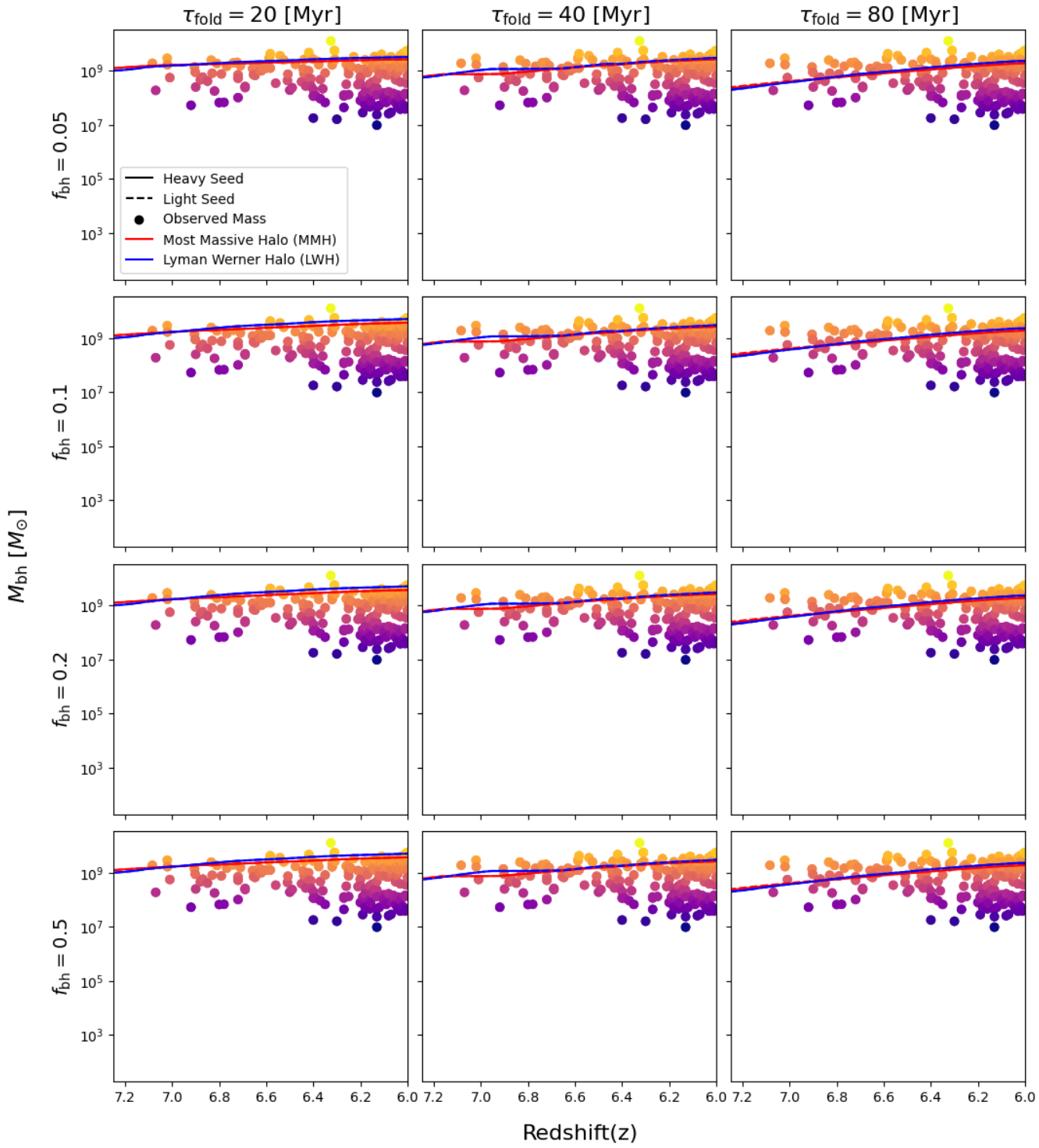

Figure 9. This figure illustrates the growth of supermassive black holes (SMBHs) with heavy and light seed masses over a redshift range of $z \in [7.1, 6]$. Growth rate is assumed to be super-Eddington rate.The heavy seed has a mass of $M_{bh} = 10^5$ M$\odot$, while the light seed has a mass of 50 M$\odot$. The growth is examined for various fractions of black hole seeds, f_{bh}, which are set to $\{0.05, 0.1, 0.2, 0.5\}$, and different efolding timescales, τ_{fold}, which are chosen from $\{20, 40, 80\}$ Myr.The growth of SMBHs in solar mass units is compared against the observed quasars compiled in Inayoshi et al. 2020.We gain valuable insights into the assembly of these massive cosmic objects.

REFERENCES

Abramowicz M. A., Fragile P. C., 2013, Living Reviews in Relativity, 16, 1
Alvarez M. A., Wise J. H., Abel T., 2009, The Astrophysical Journal, 701, L133
Becerra F., Greif T. H., Springel V., Hernquist L. E., 2015, Monthly Notices of the Royal Astronomical Society, 446, 2380
Becerra F., Marinacci F., Bromm V., Hernquist L. E., 2018, Monthly Notices of the Royal Astronomical Society, 480, 5029
Behroozi P., Wechsler R. H., Hearin A. P., Conroy C., 2019, Monthly Notices of the Royal Astronomical Society, 488, 3143
Bromm V., 2013, Reports on Progress in Physics, 76, 112901
Bromm V., Loeb A., 2003, The Astrophysical Journal, 596, 34
Chen P., Wise J. H., Norman M. L., Xu H., O'Shea B. W., 2014, The Astrophysical Journal, 795, 144
Chon S., Hirano S., Hosokawa T., Yoshida N., 2016, The Astrophysical Journal, 832, 134
Dijkstra M., Haiman Z., Mesinger A., Wyithe J. S. B., 2008, Monthly Notices of the Royal Astronomical Society, 391, 1961
Fan X., et al., 2006, The Astronomical Journal, 131, 1203
Greif T. H., 2015, Computational Astrophysics and Cosmology, 2, 1
Hosokawa T., Omukai K., Yoshida N., Yorke H. W., 2011, Science, 334, 1250
Hosokawa T., Omukai K., Yorke H. W., 2012, The Astrophysical Journal, 756, 93
Hunter J. D., 2007, Computing in Science & Engineering, 9, 90
Inayoshi K., Omukai K., Tasker E., 2014, Monthly Notices of the Royal Astronomical Society: Letters, 445, L109
Inayoshi K., Haiman Z., Ostriker J. P., 2016, Monthly Notices of the Royal Astronomical Society, 459, 3738
Inayoshi K., Visbal E., Haiman Z., 2020, Annual Review of Astronomy and Astrophysics, 58, 27
Jeon M., Pawlik A. H., Greif T. H., Glover S. C., Bromm V., Milosavljević M., Klessen R. S., 2012, in AIP Conference Proceedings. pp 325–328
Jiang Y.-F., Stone J. M., Davis S. W., 2014, The Astrophysical Journal, 796, 106
Johnson J. L., Bromm V., 2007, Monthly Notices of the Royal Astronomical Society, 374, 1557
King A., 2015, Monthly Notices of the Royal Astronomical Society: Letters, 456, L109
Latif M., Schleicher D., Schmidt W., Niemeyer J., 2013, Monthly Notices of the Royal Astronomical Society, 436, 2989
Latif M. A., Schleicher D. R., Hartwig T., 2016, Monthly Notices of the Royal Astronomical Society, 458, 233
Maio U., Borgani S., Ciardi B., Petkova M., 2019, Publications of the Astronomical Society of Australia, 36, e020
Massonneau W., Volonteri M., Dubois Y., Beckmann R. S., 2022, arXiv preprint arXiv:2201.08766
Milosavljević M., Couch S. M., Bromm V., 2009, The Astrophysical Journal, 696, L146
Mortlock D. J., et al., 2011, Nature, 474, 616
O'Shea B. W., Abel T., Whalen D., Norman M. L., 2005, The Astrophysical Journal, 628, L5
Omukai K., 2001, The Astrophysical Journal, 546, 635
Omukai K., Nishi R., 1998, The Astrophysical Journal, 508, 141
Omukai K., Palla F., 2003, The Astrophysical Journal, 589, 677
Omukai K., Hosokawa T., Yoshida N., 2010, The Astrophysical Journal, 722, 1793
O'Shea B. W., Wise J. H., Xu H., Norman M. L., 2015, The Astrophysical Journal Letters, 807, L12
Regan J. A., Haehnelt M. G., 2009, Monthly Notices of the Royal Astronomical Society, 396, 343
Regan J. A., Johansson P. H., Wise J. H., 2014, The Astrophysical Journal, 795, 137
Scoggins M. T., Haiman Z., Wise J. H., 2023, Monthly Notices of the Royal Astronomical Society, 519, 2155
Shang C., Bryan G. L., Haiman Z., 2010, Monthly Notices of the Royal Astronomical Society, 402, 1249
Smith B. D., Regan J. A., Downes T. P., Norman M. L., O'Shea B. W., Wise J. H., 2018, Monthly Notices of the Royal Astronomical Society, 480, 3762
Svestka Z., 1972, Annual Review of Astronomy and Astrophysics, 10, 1
Sądowski A., Narayan R., Tchekhovskoy A., Abarca D., Zhu Y., McKinney J. C., 2014, Monthly Notices of the Royal Astronomical Society, 447, 49
Tang J.-J., et al., 2019, Monthly Notices of the Royal Astronomical Society, 484, 2575
Toyouchi D., Inayoshi K., Hosokawa T., Kuiper R., 2021, The Astrophysical Journal, 907, 74
Tristram M., Ganga K., 2007, Reports on Progress in Physics, 70, 899
Umeda H., Yoshida N., Nomoto K., Tsuruta S., Sasaki M., Ohkubo T., 2009, Journal of Cosmology and Astroparticle Physics, 2009, 024
Wang J.-M., Chen Y.-M., Hu C., 2006, The Astrophysical Journal, 637, L85
Whalen D., Abel T., Norman M. L., 2004, The Astrophysical Journal, 610, 14
Wise J. H., Turk M. J., Abel T., 2008, The Astrophysical Journal, 682, 745
Wise J. H., Regan J. A., O'Shea B. W., Norman M. L., Downes T. P., Xu H., 2019, Nature, 566, 85
Woosley S. E., Heger A., Weaver T. A., 2002, Reviews of modern physics, 74, 1015
Wu X.-B., et al., 2015, Nature, 518, 512
Xu H., Wise J. H., Norman M. L., 2013, The Astrophysical Journal, 773, 83
Yoshida N., Omukai K., Hernquist L., 2008, Science, 321, 669